

# On the use of spatial ecology tools to characterise the evolution of the fracture process zone during quasi-brittle failure

David GRÉGOIRE, Vincent LEFORT, Gilles PIJAUDIER-CABOT

UNIV PAU & PAYS ADOUR / E2S UPPA / ISABTP,  
Laboratoire des Fluides Complexes et leurs Réservoirs,  
LFCR-IPRA, UMR5150  
64600 ANGLET, France  
david.gregoire@univ-pau.fr

## Abstract

*The degradation of quasi-brittle materials encompasses micro-cracks propagation, interaction and coalescence in order to form a macro-crack. These phenomena are located within the Fracture Process Zone (FPZ). This paper aims at providing a further insight in the description of the FPZ evolution with the help of statistical analysis of damage.*

## Keywords

Fracture, Quasi-brittle materials, Fracture process zone, Boundary effect, Mesoscopic model, Experimental, Acoustic emission, Ripley's functions.

## 1 Introduction

Fracture of quasi-brittle materials such as concrete or rocks is characterized by a macro crack surrounded by a damage zone. At the tip of the macro crack and ahead lies the so-called Fracture Process Zone (FPZ) which is a region of the material undergoing distributed damage. The size of the FPZ in these heterogeneous materials is large enough to influence the mechanical behaviour of the structure significantly. It does not depend on the structural size, but it is rather controlled by the local heterogeneities in the material as well as by the geometry of the specimen and the stress conditions. Therefore, size effect, understood here as the dependence of the dimensionless nominal strength of a structure on its size, is observed (e.g. when geometrically similar structures are compared, see for example [1]).

The purpose of this paper is to provide a further insight in the description of failure with the help of statistical analyses of damage. The statistical analysis relies on the implementation of Ripley's functions [2], which have been developed in order to exhibit patterns in image analyses.

Only the global strategy is presented in this paper. For further details, the reader may refer to reference [3]. This paper is organized as follows : section 2 shows how Ripley's function may be used in the context of damage mechanics to extract a correlation length between damage events. Section 3 recalls briefly the lattice model used in this paper. Section 4 presents the comparison between the evolution

of extracted correlation length during mesoscale numerical simulations and experimental three point bending tests where damage events are localized by acoustic emission techniques. Finally, numerical investigations of correlation length evolutions upon failure are presented in section 5 for both direct tension and three point bending specimens. Results show that the computed correlation length is not constant during failure and significant differences may be observed depending on the type of loading applied to the same specimen.

## 2 Ripley's functions applied to damage mechanics

Ripley's  $K$  function proposed in Ref. [2] is a tool for analyzing completely mapped spatial point process data, i.e. data on the locations of events [4]. Particularly, it is used to characterize the randomness in the spatial spreading of point distributions. It is of high interest in spatial ecology and has been used to characterize the development and spreading of different patterns, such as cell migration [2], tree [5] and plant [6] dissemination or disease spreading [7]. Recently, Tordesillas *et al.* [8] extended this pattern characterization method to non-biological system to analyze diffuse granular failure. In this paper, we will use the Ripley's  $K$  function to characterize the interactions and the correlations induced by damage localization in quasibrittle fracture. The Ripley's  $K$  function may be adapted to study one, two or three-dimensional spatial data, but most of the developments have been performed in 2D, which will also be the case hereafter. For a spatial point distribution, the Ripley's  $K$  function may be defined as the ratio between the density of events and the mean number of events within a distance  $r$  of any chosen event in the distribution :

$$K(r) = \frac{1}{N\rho} \sum_{i \in \mathcal{P}} \sum_{j \in \mathcal{P}} e_{ij} H(i, j, r)$$

$$\text{and } H(i, j, r) = \begin{cases} 1 & \text{if } D(i, j) \leq r \\ 0 & \text{if } D(i, j) > r \end{cases} .$$
(1)

In Eq. 1,  $N$  is the total number of points,  $\rho$  is the point density,  $\mathcal{P}$  is the point distribution and  $D(i, j)$  is the euclidean distance between two points  $i$  and  $j$ .  $e_{ij}$  is an edge effect correction factor, which is introduced to take into account that, for points located near the boundary of the study area, the real number of neighbors can be underestimated because some of them may be located outside of the study area or outside the specimen (see [3] for details).

The Ripley's  $K^{\text{ran}}$  function of a perfect randomly distributed set of points is simply given by :

$$K^{\text{ran}}(r) = \pi r^2 .$$
(2)

In order to characterize the randomness of a distribution, the Ripley's  $K$  function is usually compared to this reference function  $K^{\text{ran}}$  by defining the residual function  $L$  as :

$$L(r) = \sqrt{\frac{K(r)}{\pi}} - \sqrt{\frac{K^{\text{ran}}(r)}{\pi}} = \sqrt{\frac{K(r)}{\pi}} - r .$$
(3)

Within this definition, and for a randomly distributed set of points, the residual function stays equal to zero. Thus, plotting the residual  $L$  for an arbitrary point distribution may characterize the distance of this distribution to a perfect random one and then characterize the randomness of the distribution. Applying this concept to a set of damage points may lead to characterize how these damage points localize upon failure and therefore characterize the correlations between these damage points, which are related to the internal length in a nonlocal continuum setting.

The residual function estimated for a distribution of points which is localized spatially presents a maxima and the position of this maxima is directly linked to the size of the localized pattern (see [3] for details). For a given distribution of damage events with no particular shape, the position of the maximum of the residual function  $L(r)$  is defined as the correlation length of the distribution. Thereby, this correlation length may be extracted directly from the evolution of the residual function.

### 3 Lattice model description

A 2D plane-stress lattice model is used to characterize the correlations involved during failure in quasi-brittle materials. Practically, the lattice model is used to monitor an evolving population of damage events (a damage event corresponds to a lattice element undergoing damage during a load step), which is analyzed at each load step with the correlation length extraction method presented in part 2 and based on Ripley function applied to damage mechanics. This lattice model is based on the numerical framework proposed by Grassl and Jirasek [9]. It has been shown in previous study that this mesoscale approach is capable not only to provide consistent global responses (e.g. Force v.s. CMOD responses) [10, 11] but also to capture the local failure process realistically [11]. The lattice is made of beam elements and idealizes the meso-structure of concrete as a set of three different components : *aggregates*, *matrix* and the *interface* between them (Fig 1). The reader may refer to references [9, 10, 11] for further details.

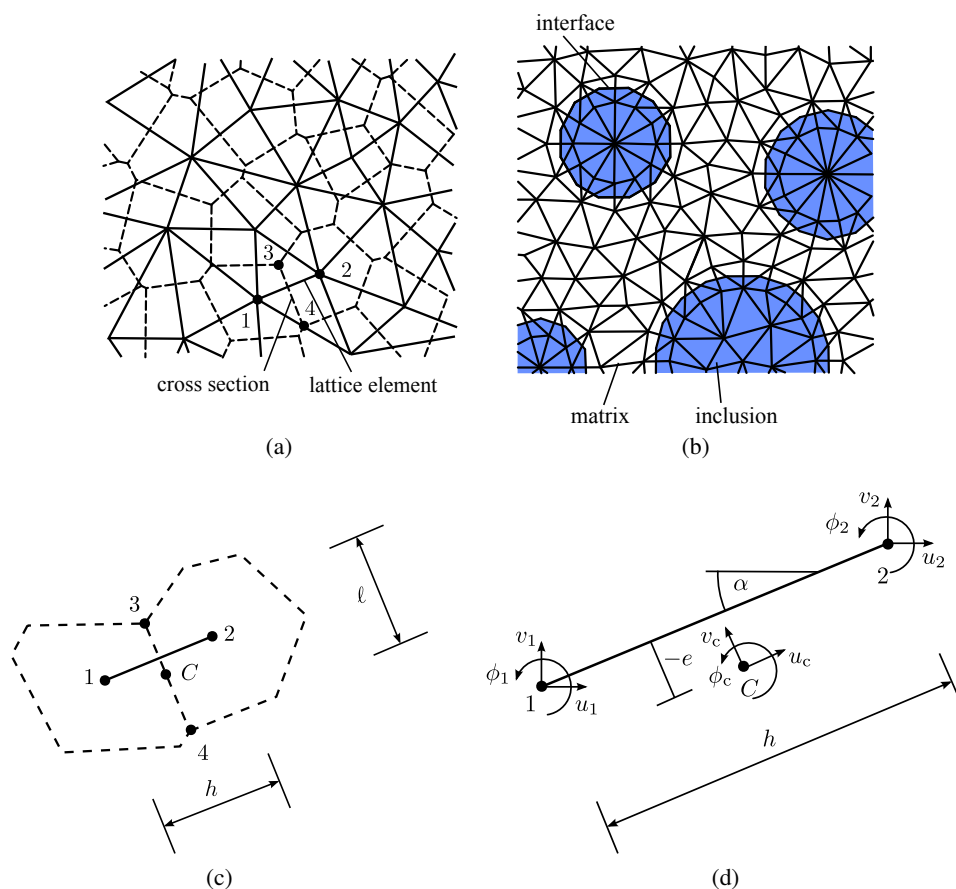


FIGURE 1 – (a) Set of lattice elements (solid lines) with middle cross-sections (dashed lines) obtained from the Voronoi tessellation of the domain. (b) Arrangement of lattice elements around aggregates (inclusions); (c) and (d) Lattice element in the global coordinate system (Reproduced from [10]).

## 4 Model validation by experimental comparisons of correlation length evolutions

Three-point bending tests were performed on geometrically similar notched and unnotched specimens made of the same concrete material. The experimental results presented hereafter are obtained from a campaign already presented by Grégoire *et al.* [11]. This campaign is similar to the one previously presented by Grégoire *et al.* [1] and includes the localisation of acoustic events during fracture additionally. The experimental procedure is briefly presented in this section. The reader may refer to references [1, 11] for further details.

The concrete formulation used here is based on a ready-mix concrete mixture obtained from Unibeton (<http://www.unibeton.fr>). Detailed gradings of the sand, the aggregates and the mix are given in [1]. After demolding, the specimens were stored under water at 20°C. The characterization of their mechanical properties was made by compression and splitting (Brazilian) tests according to European standards (EN 12390-1-3-6). The testing rig used for the bending tests was a three-point bending setup on a servo-hydraulic testing machine (HB250, Zwick/Roell). During the tests, acoustic events were recorded and localised. The AE system used in this study comprised an eighth-channel MISTRAS system, a general purpose interface bus (PCI-DISP4) and a PC for data storage analysis. Four acoustic transducers (resonant frequency of 150 kHz) were placed around the expected location of the crack, on one side of specimen. The AE event localisation program relies on time of flight analysis and triangulation.

Figure 2 shows the results of the cumulative locations of the acoustic events for two half-notched and fifth-notched beams (depth  $D=200\text{mm}$ ). The plotted points indicate the detected AE sources over the observation window centered at the notch. Events carry different energies and we have plotted here all the events. The warmer/darker the marker of one event, the higher the acoustic energy (color/black&white). One can filter the events and retain only those with a sufficiently large acoustic energy. These events should correspond to the macrocrack propagating in the specimen.

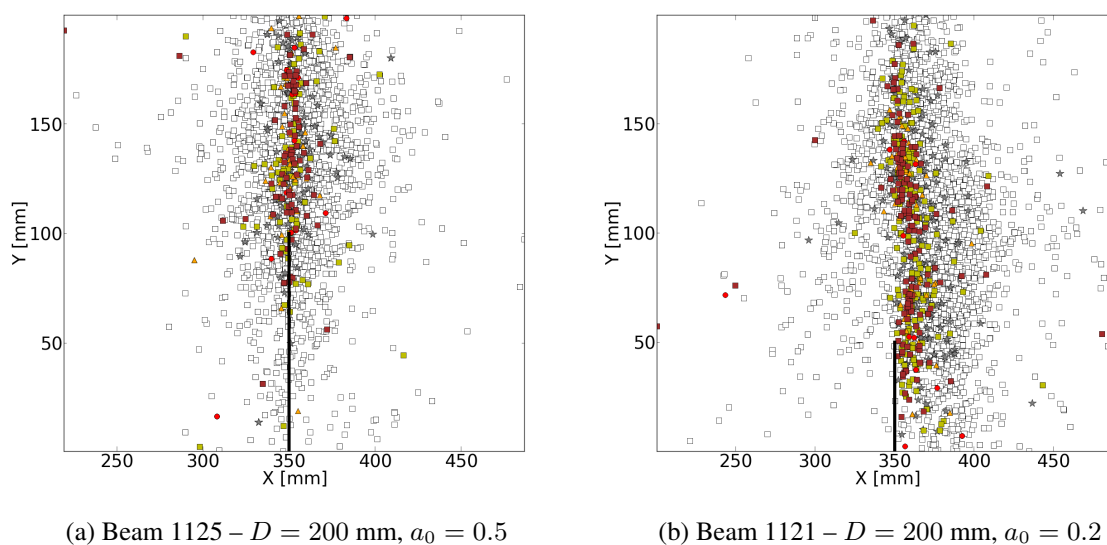


FIGURE 2 – Distribution of acoustic events in different geometries of beam – map of distribution of energies. Reproduced from [11].

Experimentally, a damage event is associated to a material point producing acoustic emissions upon failure, which have been detected and then localized by at least three acoustic sensors during a load step. Numerically, a damage event is associated to a lattice material point (Point  $C$  in figure 1.d) undergoing damage during a load step.

A minimum number of damage events has to be captured to perform the post-processing. Numerically there is almost no limitation because a lot of damage events are acquired within a loading step. Experimentally, the acoustic emission is much more restrictive because only few acoustic events may be acquired by the technique, especially in the nonlinear pre-peak regime. Therefore, the loading curve discretization is determined to ensure to capture enough events experimentally in order to achieve a statistically representative post-processing. Since the first goal of this section is to test the relevance of the meso-model by comparing the numerical results with experimental ones, we adopt the same interval length, which is driven by the experimental minimum. Numerical investigations on correlation length evolutions upon failure based on a finer loading curve discretization are presented alone in part 5.

Numerically, the space discretization corresponds intrinsically to the lattice discretization. Experimentally, there is an implicit space discretization due to the acoustic sensor resolution and the acoustic emission localization technique resolution. This resolution is of the order of 4 mm [11]. This means that two acoustic emissions produced at two different material points separated by a distance smaller than this resolution may not be distinguished. This means also that all the acoustic emissions produced in the corresponding vicinity of a material point are seen by the acoustic sensors as a single acoustic emission with an acoustic energy corresponding to the addition of all the individual acoustic energies. Therefore the numerical and experimental data cannot be directly compared since the Ripley's function post-processing is only based on the spatial repartition of a given distribution of point. Experimentally, an acoustic event will count for a single data point in the Ripley's function analysis even if, locally, several material points undergo damage and produce acoustic emissions. This is overcome by taking into account the intensity of the energy dissipated during each damage event in the post-processing by Ripley's functions. Assuming that the acoustic energy recorded for each event is proportional to the energy dissipated during the corresponding damage event, it is possible to compare experimental and numerical results in term of dissipated energy (see [3] for details).

Figure 3 presents the comparison between experimental and numerical extracted correlation length with intensity conversion. The correlation length is extracted based on the analysis by Ripley's functions as presented in section 2. Even if an important scattering is observed on the experimental data, we observe a global good agreement between the experimental and the numerical results. This means that the numerical model and the Ripley's post-processing procedure may be used alone to investigate the evolution of the correlation length upon failure.

## **5 Numerical investigations of correlation length evolutions upon failure**

### **5.1 Response in direct tension**

In this subsection, the correlation length extraction method is applied to a direct tension test. We consider a concrete specimen presenting the same characteristics than the one previously studied.

This correlation length is directly related to the size of the damage zone and therefore to the internal length in a nonlocal continuum setting. The evolution of the extracted correlation length is presented in

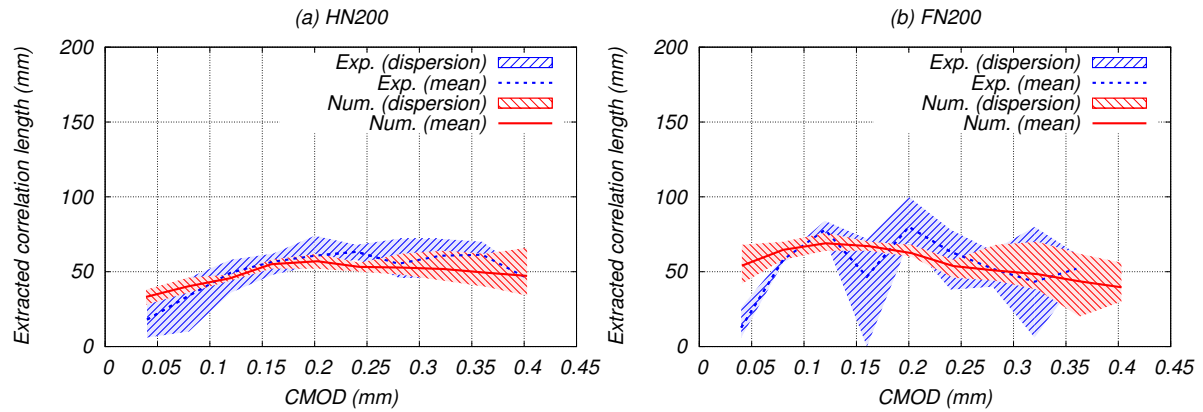


FIGURE 3 – Comparison between experimental and numerical extracted correlation length with intensity conversion. Reproduced from [3].

figure 4.b. In concrete, damage develops at the interface between aggregates and mortar. At the beginning of the test, damage develops and spreads all over the specimen and then the correlation length grows and it would reach eventually the size of the box. However, at  $CMOD \approx 0.01$  mm, damage starts to localize within a fracture process zone surrounding the pre-notch tip and the correlation length reaches a plateau. Later on, and as the fracture process zone develops to form a macro-crack, the correlation length decreases. When the macro-crack is fully developed, surrounded by the fracture process zone, the correlation length reaches a new plateau at a value corresponding to four times the larger aggregate size ( $\approx 10$  mm).

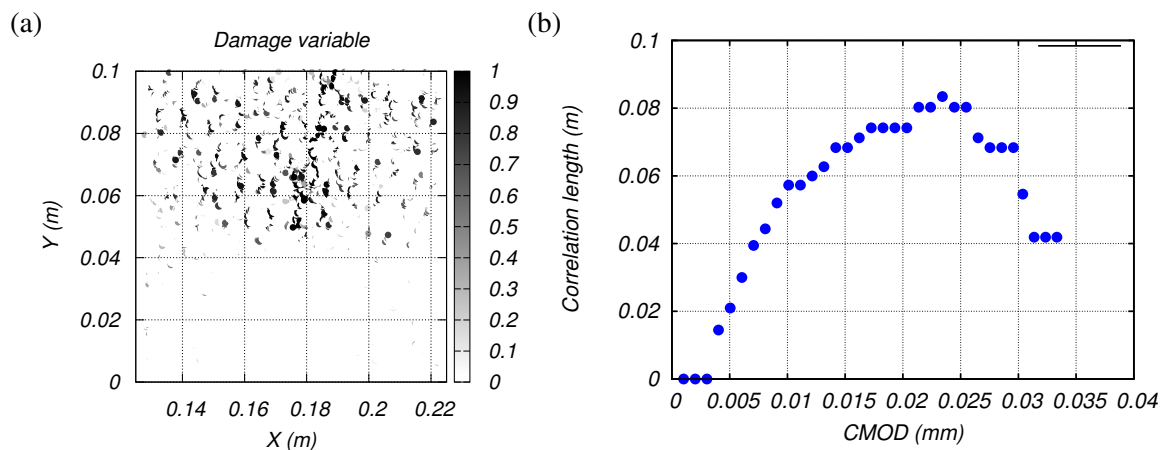


FIGURE 4 – Distribution of damage events for a direct tension test (a) and corresponding correlation length evolution (b). Reproduced from [3]

## 5.2 Response in bending

In this subsection, the correlation length extraction method is applied to the three point bending beams presented in section 4. We compare here the response of long notch and unnotched specimens with a depth of 100 mm. The same post processing method is applied : the test are CMOD controlled and at each CMOD step, the distribution of incremental damage events is plotted (see figure 5.a-b) and the corresponding Ripley's residual function is estimated. The correlation length is extracted based on the analysis by Ripley's functions as presented in section 2. The evolution of the extracted correlation length is presented in figure 5.c.

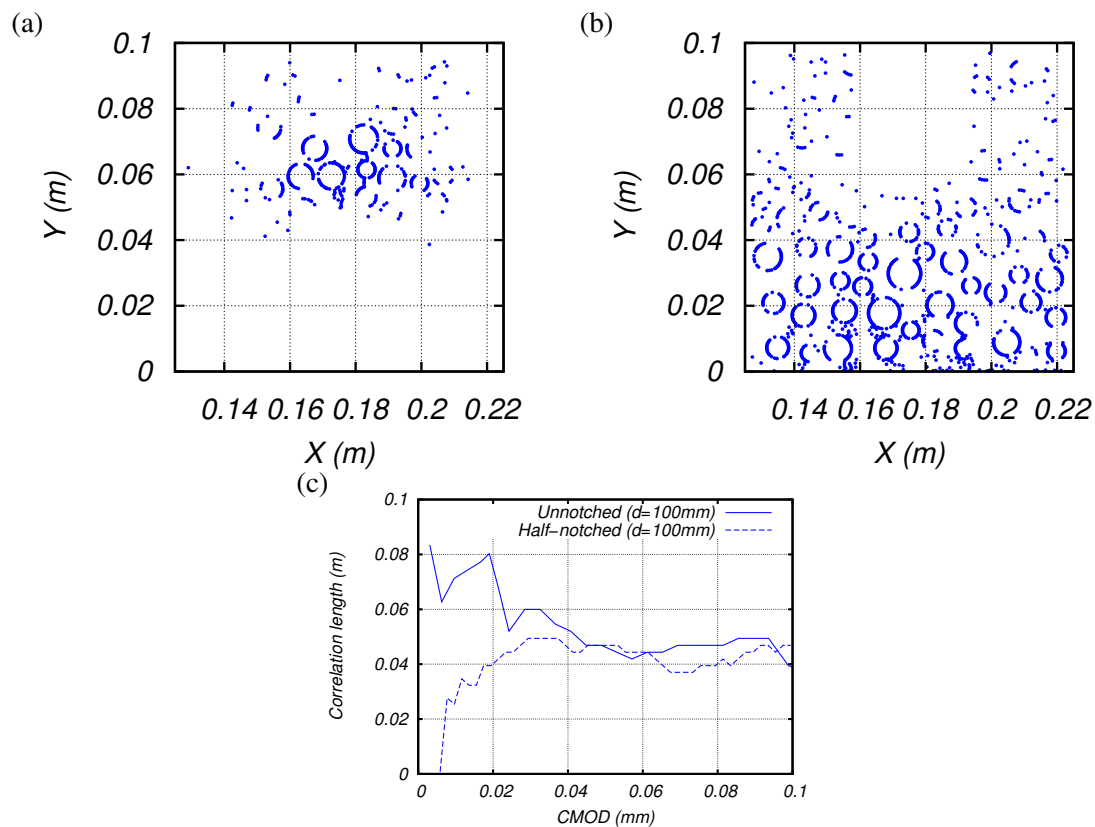


FIGURE 5 – Responses in bending : (a) Damage distribution at peak for the long notch specimen ; (b) Damage distribution at peak for the unnotched specimen ; (c) Evolution of the extracted correlation lengths for both specimen. Reproduced from [3]

For the notched specimen, the evolution of damage is similar to what has been observed in direct tension. The pre-notch triggers the damage localization and the correlation length grows to reach a plateau at a value corresponding to four/five times the larger aggregate size ( $\approx 10$  mm). However, during the initiation of failure, damage does not spread over the whole specimen because of the bending strain gradient. That is the reason why only a growing phase is observed before the plateau. For the unnotched specimen, the damage evolution is totally different. Since there is no pre-notch, the damage localization is not triggered and damage spreads on the bottom surface of the specimen. Therefore, the correlation length is equal to the analysis box size at the beginning at damage initiation. At some point, a macro-crack will emerge from the bottom face and propagate surrounded by a fracture process zone. The correlation length is decreasing from the analysis box size to reach the same plateau observed for a notched specimen at a value corresponding to four/five times the larger aggregate size ( $\approx 10$  mm).

## 6 Concluding remarks

We have presented a detailed analysis based on Ripley's functions of the cracking process at the meso-scale of concrete specimen, both numerically and experimentally. The computational model is a lattice-based approach which already proved to be able to capture size effect test data for notched and unnotched bending beams and the force v.s. CMOD response as well (see [10]). Moreover, comparison with experiments coupled with acoustic emission analyses proved also that the mesoscale model is representative of the local process of quasi-brittle failure in terms of dissipative energy maps and histograms of relative distances between damage events (see [11]).

The following concluding statements can be made :

- The post processing with Ripley's function provides indicators of the randomness of a distribution of events.
- It has been shown that a correlation length, which may possibly be linked to an internal length in the sense of non local models, may be extracted from the Ripley's function analyse applied to damage mechanics. However, the exact correspondance between the extracted correlation length and a nonlocal model internal length remains to be derived.
- The evolutions of this extracted correlation length upon failure have been presented. Comparisons between numerical data based on mesoscale lattice modeling and experimental data where damage events were localized by acoustic emission techniques were performed. Even if an important scattering is observed on the experimental data, we observed a global good agreement between the experimental and the numerical results. This means that the numerical model and the Ripley's post-processing procedure may be used alone to investigate the evolution of the correlation length upon failure.
- Numerical investigations have been performed on both direct tension and three point bending specimens. The results show that the extracted correlation length is not constant during failure and significant differences may be observed depending on the type of loading applied to the same specimen.

This conclusion opens the path for further analyses of the fracture process, solely based on numerical analyses with the mesoscale model. From these studies, a better understanding of the correlations between damage events, that should result into non local continuum modeling at the macroscale, is expected.

## Acknowledgments

Financial support from TOTAL Exploration & Production under the project "Fracture and permeability of heterogeneous quasi-brittle materials" is gratefully acknowledged. The authors wish also to acknowledge the University of Bordeaux for the use of the cluster AVAKAS. David Grégoire and Gilles Pijaudier-Cabot are fellows of the *Institut Universitaire de France*.

## Références

- [1] D. Grégoire, L. B. Rojas-Solano, G. Pijaudier-Cabot, Failure and size effect for notched and unnotched concrete beams, *Int. J. Numerical and Analytical Methods in Geomechanics* 37 (10) (2013) 1434–1452.
- [2] B. D. Ripley, Modelling Spatial Patterns, *Journal of the Royal Statistical Society. Series B (Methodological)* 39 (2) (1977) 172–212.
- [3] V. Lefort, G. Pijaudier-Cabot, D. Grégoire, Analysis by ripley's function of the correlations involved during failure in quasi-brittle materials : Experimental and numerical investigations at the mesoscale, *Engineering Fracture Mechanics* 147 (2015) 449 – 467.
- [4] P. M. Dixon, Ripley's K function, in : A. H. El-shaarawi, W. W. Piegorsch (Eds.), *Encyclopedia of Environmetrics*, volume 3, Vol. 3, John Wiley & Sons, Ltd., Chichester, 2002, pp. 1796–1803.
- [5] R. P. Duncan, Flood Disturbance and the Coexistence of Species in a Lowland Podocarp Forest, South Westland, New Zealand Author(s) :, *Journal of Ecology* 81 (3) (1993) 403–416.



- 
- [6] N. E. Stamp, J. R. Lucas, Spatial Patterns and Dispersal Distances of Explosively Dispersing Plants in Florida Sandhill Vegetation, *Journal of Ecology* 78 (3) (1990) 589–600.
- [7] P. J. Diggle, A. G. Chetwynd, Second-Order Analysis of Spatial Clustering for Inhomogeneous Populations, *Biometrics* 47 (3) (1991) 1155–1163.
- [8] A. Tordesillas, S. Pucilowski, L. Sibille, F. Nicot, F. Darve, Multiscale characterisation of diffuse granular failure, *Philosophical Magazine* 92 (36) (2012) 4547–4587.
- [9] P. Grassl, M. Jirásek, Meso-scale approach to modelling the fracture process zone of concrete subjected to uniaxial tension, *International Journal of Solids and Structures* 47 (7-8) (2010) 957–968.
- [10] P. Grassl, D. Grégoire, L. B. Rojas-Solano, G. Pijaudier-Cabot, Meso-scale modelling of the size effect on the fracture process zone of concrete, *International Journal of Solids and Structures* 49 (13) (2012) 1818–1827.
- [11] Grégoire, D. and Verdon, L. B. and Lefort, V. and Grassl, P. and Saliba, J. and Regoin, J.-P. and Loukili, A. and Pijaudier-Cabot, G., Mesoscale analysis of failure in quasi-brittle materials : comparison between lattice model and acoustic emission data, *International Journal of Numerical and Analytical Methods in Geomechanics* (2015) doi : 10.1002/nag.2363.